REPORT DOCUMENTATION PAGE

Form Approved
OMB No. 0704-0188

1. REPORT DATE *(DD-MM-YYYY)*	2. REPORT TYPE	3. DATES COVERED *(From - To)*
10-19-2009	Final Technical Report	28 Dec 2006 - 30 Sep 2009

4. TITLE AND SUBTITLE
Advanced Microwave Ferrite Research (AMFeR): Phase Four

5a. CONTRACT NUMBER

5b. GRANT NUMBER
N00014-07-1-0476

5c. PROGRAM ELEMENT NUMBER

6. AUTHOR(S)
Young, Jeffrey L.

5d. PROJECT NUMBER

5e. TASK NUMBER

5f. WORK UNIT NUMBER

7. PERFORMING ORGANIZATION NAME(S) AND ADDRESS(ES)
University of Idaho, Office of Sponsored Programs
Morrill Hall Room 414
PO Box 443020
Moscow, ID 83844-3020

8. PERFORMING ORGANIZATION REPORT NUMBER

9. SPONSORING/MONITORING AGENCY NAME(S) AND ADDRESS(ES)
Office of Naval Research
One Liberty Center
875 N. Randolph Street, Suite 1425
Arlington, VA 22203-1995

10. SPONSOR/MONITOR'S ACRONYM(S)
ONR

11. SPONSORING/MONITORING AGENCY REPORT NUMBER
PR# 09PR07767-00

12. DISTRIBUTION AVAILABILITY STATEMENT
Unlimited

13. SUPPLEMENTARY NOTES

14. ABSTRACT
The purpose of this research endeavor is to devise ferrite materials for microwave, self-biased circulator applications. To this end, the research team focused on two key activities. The first was the development of a ferrite/epoxy composite that can be directly injected into a dielectric substrate. As the ferrite cured, two external magnets were placed on both sides of the ferrite to align the ferrite moments; once cured, the moments were locked in place to form a self-bias structure. Microstrip traces were patterned on it to form a microstrip circuit. Frequency-swept S-parameters measurements were made to ascertain the device's response. On average, the device exhibited excellent return loss and isolation on the order of 20 dB or more over a narrow band of 1 GHz centered at 25GHz. However, the insertion losses were unacceptable at about 11.7 dB. This latter outcome is directly related to the large linewidths. In addition to fabricating our own ferrites, we also employed strontium-ferrites that were fabricated by Countis Laboratories. These ferrites exhibit stronger crystalline anisotropies than their barium-ferrite cousins, but are nevertheless suitable for this application. When used in a self-biased circulator, the response of the circulator was marginally acceptable.

15. SUBJECT TERMS
self-biased ferrites, circulators, matching schemes

16. SECURITY CLASSIFICATION OF:			17. LIMITATION OF ABSTRACT	18. NUMBER OF PAGES	19a. NAME OF RESPONSIBLE PERSON
a. REPORT	b. ABSTRACT	c. THIS PAGE	UU	26	Jeffrey L. Young
U	U	U			19b. TELEPONE NUMBER *(Include area code)* 208-885-6829

Final Report

Advanced Microwave Ferrite Research (AMFeR): Phase Four

Dr. Jeffrey L. Young
MRC Institute/Electrieal and Computer Engineering
University of Idaho
Moscow, ID 83844-1024
208-885-6829
jyoung@mrc.uidaho.edu

October 15, 2009

Supporting Information:

Grant Number: N00014-07-1-0476

Original Contract Period: December 26, 2006 through June 30, 2008
Extended Contract Period: July 1, 2008 through September 30, 2009

FY06 Funded Amount: $875,000

Executive Summary:

Described herein are the key findings and results associated with the Advance Microwave Ferrite Research (AMFeR), Phase IV project. As quoted in the Phase III report "The purpose of this research endeavor is to devise ferrite materials for microwave, self-biased circulator applications. Materials suitable for this study are the class of M-type, hexagonal ferrites, which typically have large crystalline anisotropies that tend align the magnetic moments of the ferrite in a single direction with the hope of achieving a quasi-saturated state. In addition to having large crystalline anisotropy, the materials must also possess large magnetic coercivities that keep the ferrite saturated even in the presence of a strong, shape-dependent demagnetization field. As a rule of thumb, the coercivity should be of the same strength (or greater) as the magnetic saturation to achieve self-bias operation. The central task of the project is to fabricate ferrites that have a high magnetic saturation, high coercivity and low FMR linewidth"

To this end, the AMFeR team focused on two key activities. The first was the development of a ferrite/epoxy composite that can be directly injected into a dielectric substrate. As the ferrite cured, two external magnets were placed on both sides of the ferrite to align the ferrite moments; once cured, the moments were locked in place to form a self-bias structure. Data obtained from a vibrating sample magnetometer (VSM) substantiated this claim as seen in typical coercivity data of 4,006 Oe and saturation data of 1,872 G. Linewidth measurements were difficult to make due to nondescript ferromagnetic resonant peaks. This effectively suggests that the resulting ferrite is high loss at microwave frequencies.

Once the ferrite was fully cured, microstrip traces were patterned on it to form a microstrip circuit. Frequency-swept S-parameters measurements were made to ascertain the device's response. On average, the device exhibited excellent return loss and isolation on the order of 20 dB or more over a narrow band of 1 GHz centered at 25GHz. However, the insertion losses were unacceptable at about 11.7 dB. This latter outcome is directly related to the large linewidths, as noted previously.

In addition to fabricating our own ferrites, we also employed strontium-ferrites that were fabricated by Countis Laboratories. These ferrites exhibit stronger crystalline anisotropies than their barium-ferrite cousins, but are nevertheless suitable for this application. When used in a self-biased circulator, the response of the circulator was marginally acceptable. At the tuned frequency of 23.45 GHz the return loss and the isolation were about 50 dB and the insertion loss was 3.5dB. The fact that the insertion loss was decent correlates well to the measured linewidth of 1,862 Oe at 59.5 GHz.

An auxiliary activity was sponsored to support Colorado State University (Prof. Carl Patton, PI), who partnered with UI in the fabrication and validation of a Ferromagnetic Resonant (FMR) Linewidth System. This custom system is concurrently configured to measure FMR linewidths in the X, K, U or V bands.

The key team members of this project were divided into two functional groups: Material Science and Microwave Device Design. The Material Science Group, headed by Professors David McIlroy and Wei Jiang Yeh, was responsible for ferrite material fabrication, characterization and validation. The Microwave Device Group, headed by Professor Jeffrey Young, was responsible for device design, fabrication and test. Each group has prepared a summary report on their methods and findings; the reports are attached as appendices. The appendices are organized as follows:

Appendix A: Carla, Blengeri, Wei Jiang Yeh and David McIlroy, "Fabrication of Barium Ferrite Disks"
Appendix B: Nan Mo, Jaydip Das and Carl Patton, "FMR Spectrometer Upgrade to U-band Frequencies and Inter-laboratory Comparison at 52, 55, and 58 GHz"
Appendix C: Benton O'Neil and Jeffrey L. Young, "Experimental Investigation of a Self-Biased Microstrip Circulator" (Reprint, published in the "*IEEE Transactions on Microwave Theory and Technique*)

Journal Publications:

B. K. O'Neil and J. L. Young, "Experimental investigation of a self-biased microstrip circulator," *IEEE Transactions on Microwave Theory and Techniques,* vol. 57, no. 7, pp. 1669-1674, 2009.

B. O'Neil and J. L. Young, "Evaluation of coplanar waveguide-to-microstrip transitions for precision S-parameter measurements," *Microwave and Optical Technology Letters*, vol. 50, no. 10, pp. 2667-2671, October 2008.

Conference presentations:

B. O'Neil and J.L. Young (Invited), "Design of self-biased, wideband circulators for integrated antenna systems," Special Session: Enabling Technology for Multifunctional and Interoperable Communications Systems: Reconfigurable Antennas and RF Front Ends, *IEEE Antennas and Propagation International Symposium and USNC/URSI National Radio Science Meeting*, San Diego, California, July 2008.

W. J. Yeh, Carla Blengeri, Aditya Abburi, David N. McIlroy, "Synthesis of C-Axis Barium Hexaferrite Puck for Communication Application," *Seventh International conference on New Theories, Discoveries and Applications Superconductors and Related Materials,* Beijing, China, May 2009,

Appendix A

Fabrication of Barium Ferrite Disks

Ms. Carla Blengeri, Dr. Wei Jiang Yeh and Dr. David McIlroy
Department of Physics, University of Idaho

I. Abstract

In the present work a novel composite material consisting of $BaFe_{12}O_{19}$ nanopowder and an epoxy binder is evaluated as a low cost solution for self-biased circulator applications. The resulting barium ferrite mixture is pressed into a dielectric substrate hole to form the basis of a self-biased microwave circulator; copper microstrip transmission lines are patterned onto the substrate and ferrite to form the remaining parts of the circulator. The ferrite mixture exhibits good magnetic properties. For example, magnetization saturation is between 2,000 to 2,500 G, perpendicular coercivity ranges from 3,800 to 4,000 Oe and a typical squareness of approximately 0.9. The measured circulator response is 28.5 dB for isolation, 11.5 dB for insertion loss and 12.7 dB for return loss.

II. Introduction

The chemical stability and large uniaxial crystalline anisotropies of highly oriented hexagonal M-type ferrites, such as $BaFe_{12}O_{19}$ (BaM), have led researchers to consider their use in self-biased, microwave circulator applications. Magnetic saturation is achieved by the equivalent anisotropy field rather than by the traditional external biasing magnet, which is typically heavy, bulky and costly. Furthermore, the elimination of this biasing magnet also allows for the potential integration of the microwave circulator into a monolithic microwave circuit. To achieve a self-bias state, the coercivity must be greater than the saturation to counteract the influence of the shape-dependent demagnetization field. For microwave applications, ferrite thicknesses on the order of 0.5 mm are necessary.

Many methods have been used to grow c-axis oriented BaM films. These include sputtering [1], pulse laser deposition (PLD) [2], chemical vapor deposition [3], liquid phase epitaxy (LPE) [4,5] and modified liquid phase epitaxy (MLPE) [6]. Although sputtering and PLD can produce excellent c-axis oriented thin BaM films with low microwave losses [7], the maximum thickness of the films fabricated by a vacuum technique is only 30 μm. Even so, Yuan *et al.* [4] have shown that even with a slow sputtering deposition rate, films thicker than 3 μm tend to delaminate from the substrate during annealing. Oliver *et al.* [8] have used PLD to grow 28 μm BaM thick films that do not crack or delaminate. Setting these delaminating issues aside, we note that the aforementioned thicknesses are inadequate for microwave circuit applications. LPE and MLPE are the most effective way to grow BaM films thicker than 0.1 mm. Furthermore, these LPE and MLPE thick films have excellent c-axis orientation with coercivities on the order of 10-100 Oe, which indicates that they have almost single crystal structure. However, single crystal BaM films cannot be self-biased due to the weak coercivity field relative to saturations on the order 4,000 G and higher. Current research indicates that

polycrystalline c-axis orientated barium ferrite thick films with high coercivity values are the possible solution to the self-biased problem. For example, strontium hexaferrites have been used to make self-biased microwave circulators; see Oliver *et al.* [8] and O'Neil *et al.* [9]. Since both strontium and barium ferrites have similar crystal properties, it seems reasonable to conclude that the success with strontium hexaferrites [8,9] points to success with barium ferrite.

III. Proposal Objective

- Develop barium ferrite thick films to be incorporated in self-biased microwave devices.
- Integrate the barium ferrite thick film within the substrate.
- Test the RF performance of the devices.

IV. Methodology

Fabrication of the Barium Ferrite thick film

Each barium ferrite thick film is made from a combination of commercially available barium ferrite nanopowder (barium dodecairon nonadecaoxide $BaFe_{12}O_{19}$) and 30 minutes epoxy with a ratio of 80/20 respectively. The nanopowder is sifted through a 450 wire mesh. The purpose of this step is to improve the particle size in order to achieve better magnetic alignment, i.e. superior magnetic properties. After this is done the powder is weighed and placed into the mixing container followed by weighing and adding epoxy to the mix. To aid with the mixing process, 1 ml of acetone is added to the mix. The total mixing time is 3.5 minutes, where the goal is to produce a ferrite mixture with a uniform distribution of barium ferrite nanoparticles.

With the ferrite mixture so prepared, a small amount of the mixture is placed in a 1.5 cm (diameter) hole of a 0.5mm thick alumina substrate and pressed by a modified 0.5 ton press. To assure uniform alignment of the magnetic moments within the mixture, one inch diameter by one inch tall neodymium permanent magnets were mounted on the top and bottom chucks of the press. With the press closed, the magnetic field strength between the magnets is 1.2 T. The main pressing force on the mixture originates from the attraction force between the two magnets, not from the mechanical forces of the press. The sample is kept in this high magnetic field environment for 48 hours. Upon removal from the press, it is cured at room temperature for another 48 hours.

After the curing process is complete, each sample is polished using the precision lapping/polishing machine (UNIPOL-810). The polishing process was done in several steps. To remove coarse features and excess material #320 waterproof sandpaper is used first. Polishing cloth with a 3 micron polishing slurry is then employed to create a smooth surface. Finally, 0.05 micron glass polishing solution is used to fine polish both sides of the sample. To facilitate drying, the sample is placed on a hot plate at 45°C for 24 hours. This process yields a barium ferrite puck that is rigidly secured in the center hole of the substrate.

We observed on several occasions that after the drying process is concluded a very thin gap forms between the puck and the substrate. This is attributed to the contraction of the barium ferrite mixture during the curing process. This problem is remedied by using a small amount of Devcon 90 minutes epoxy as a gap filler. After this excess epoxy is removed by a dry polishing process, the sample is cured at room temperature for another 90 minutes and then placed on a hot plate for 24 hours at 45°C. The magnetic properties of the ferrite mixture are subsequently measured by a vibrating sample magnetometer (VSM).

Once the samples are cured and a visual examination is performed (visual examination is needed to make sure all the gaps were filled), each one of the samples are cleaned twice with acetone and alcohol using first regular kimwipes and then with a clean fabric wipe for a class 100 clean room. Lastly, each sample is dried with compressed air to insure that any particles on the surface are removed prior to metallization.

The finished circulator is created by sputtering a 100 nm layer of titanium to enhance adhesion, followed by a 4 μm film of copper. The ground plane is formed by sputtering Cu on the entire back surface of the circulator. The microstrip traces are formed and defined using a stainless steel stencil mask. An Ar DC plasma deposition is used to deposit the Ti and Cu layers. The depositions are done at a pressure of 8mTorr with a DC power input of 150W for titanium and 15mTorr with a DC power input of 150W for copper. At these settings, the deposition rate is 500Å/min for Ti and 0.26μm/min for Cu.

A diagram of the mask and its dimensions is shown in Figure 1. The main traces emanate from the center of the substrate at 120 degree intervals; orthogonal to these traces are another set of traces that form the impedance matching network. Figure 2 is a photograph of the finished circulator. Coaxial-to-microstrip launching pads are added at the end of each main trace to facilitate testing with a microwave network analyzer.

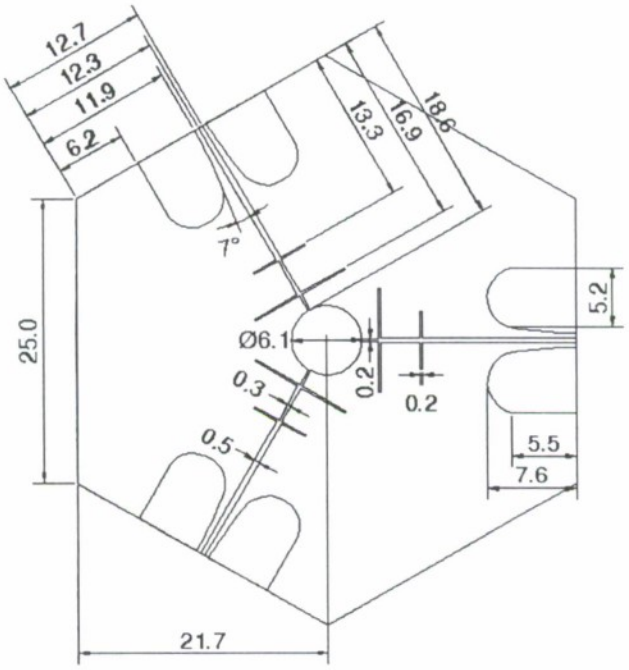

Fig.1. Diagram of the mask (dimensions in mm).

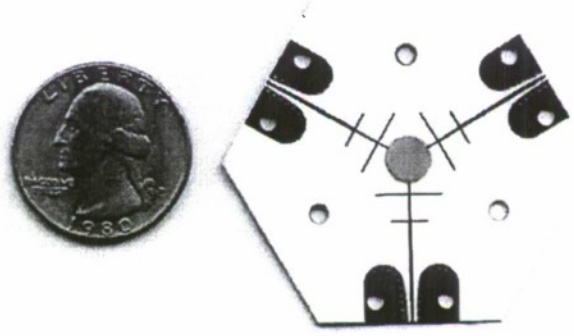

Fig. 2. A photograph of a competed barium ferrite self-biased circulator.

Magnetic Characterization of Barium Ferrite Disk

The magnetic properties of the samples were ascertained using a vibrating sample magnetometer (VSM), which takes two measurements in a 0-degree angle (out of plane) and in a 90-degree angle (in plane). Because of the size of the hexagonal substrates they cannot be placed in the VSM. To remedy this, small circular samples are made at the same time containing the same mixture as the ferrites used in the circulator. This allowed us to determine the magnetic properties of the barium ferrite disks embedded in the hexagonal substrates.

V. Results and Discussion

Over the last year the magnetic properties of different nanopowder/epoxy ratios have been tested. As it can be observed in Fig. 3, the 80/20 ratio is optimal. A 90/10 ratio was also tested, but the mixing process was difficult, i.e. the uniformity of the mixture was compromised. With the 80/20-recipe ratio we obtained a manageable and uniform mixture, which resulted in consistent magnetic properties of all samples.

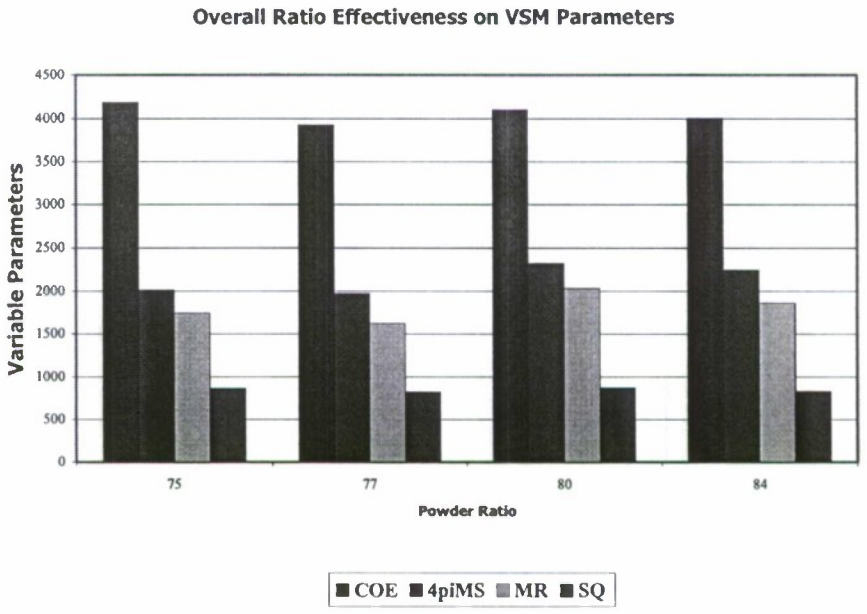

Fig. 3. VSM analysis of the magnetic properties of different nanopowder/epoxy ratios.

Representative magnetic hysteresis loops of a barium ferrite disk for in- and out-of-plane magnetic polarization are displayed in Fig. 4. The most important magnetic properties that we take into consideration are the squareness of the hysteresis loop, the coercive field, the saturation magnetization $4\pi M_s$, and the remanent magnetization MR.

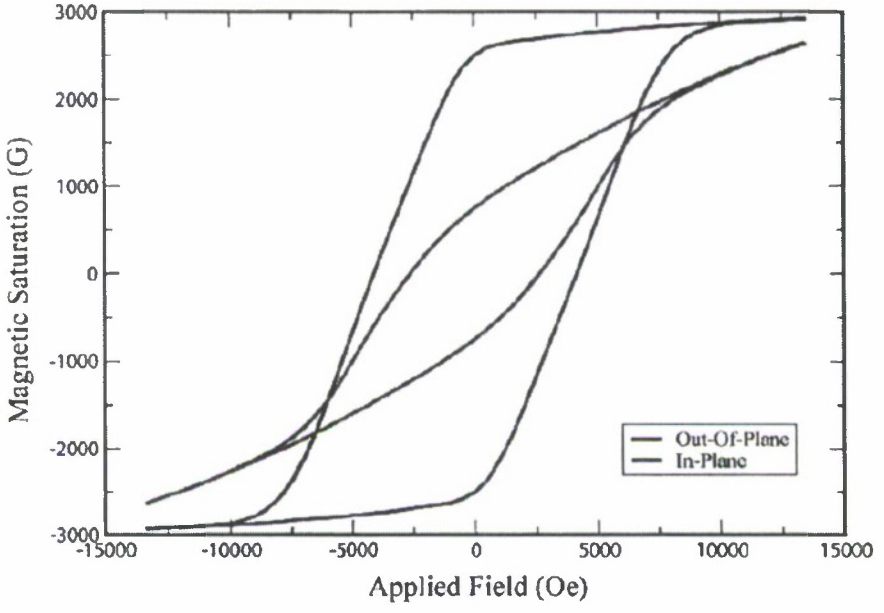

Fig. 4. VSM data for the in-plane and out-of-plane hysteresis loops for a barium ferrite thick film with 80/20 ratio

Table 1 shows the average of 200 samples with 80/20 ratio measured by the VSM. Judging by the standard deviation we see that this technique has a high rate of repeatability and consistently produces good thick disks with an average squareness of 0.83 and a mean coercivity of 4,006 Oe. Samples also have good values for the saturation magnetization with an average of 2,261 G and 1,872 G for the remanent magnetization.

	Thickness (mm)	**Squarness**	**Coercivity Field**	**Saturation Magnetization (Guass)**	**Remanent Magnetization (Guass)**
Mean (μ)	0.70	0.83	4006	2,261	1,872
STDV (σ)	0.09	0.02	233	167	141

Table 1. Value of the mean and standard deviation of 200 samples measured by the VSM

When the completed devices were measured on a microwave network analyzer, the RF signals were weak and the RF losses were large. To improve the signal from the devices,

the nanopowder was subjected to a ball milling process and sieved through a 450 mesh, which yielded an average particle size of 32 microns versus 44 microns prior to sieving. In Table 2 we can observe the comparison among the different treatments of the barium ferrite nanopowder. Process A is the initial process used prior to modifications. Process B is the same process but the powder was ball milled for a week and sieved through a 450 mesh. This process showed an improvement in all the magnetic properties except for the coercivity field, which dropped by almost 50%. Process C was done because the physical consistency of the mixture changed. In this case, the mixture was wet and less viscid; consequently, an additional 19% of powder was added. This process had almost the same result as process B; again, all the magnetic properties improved except for the coercivity field, which dropped almost 50%. Process D was executed with the same ratio but the difference relative to the other processes is that the powder was only sieved through a 450 mesh (i.e. no ball milling), which resulted in an overall improvement for the magnetic properties including the coercivity field.

Process		Sq (Mean)	Coercivity (Mean) (Oe)	$4\pi M_s$ (Mean (G)	MR (Mean) (G)
A	80/20 recipe ratio	0.83	4,003	2,262	1,870
B	80/20 recipe ratio after ball milling and sifted with 450 mesh	0.89	2,558	2,276	2,021
C	80/20 recipe ratio after ball milling and sieved with 450 Mesh plus adding 19% more powder	0.86	2,452	2,496	2,136
D	80/20 recipe ratio after sifted with 450 mesh	0.85	4,081	2,243	1,915

Table 2. Comparison among different process performed to the barium ferrite nanopowder.

RF Measurements and Properties

When placed in an RF test fixture that allowed for a connection to the microstrip traces via coaxial transitions, the final device was characterized using a microwave network analyzer that measures the S-parameters of the device as a function of frequency. Results of one such measurement are shown in Figure 5.

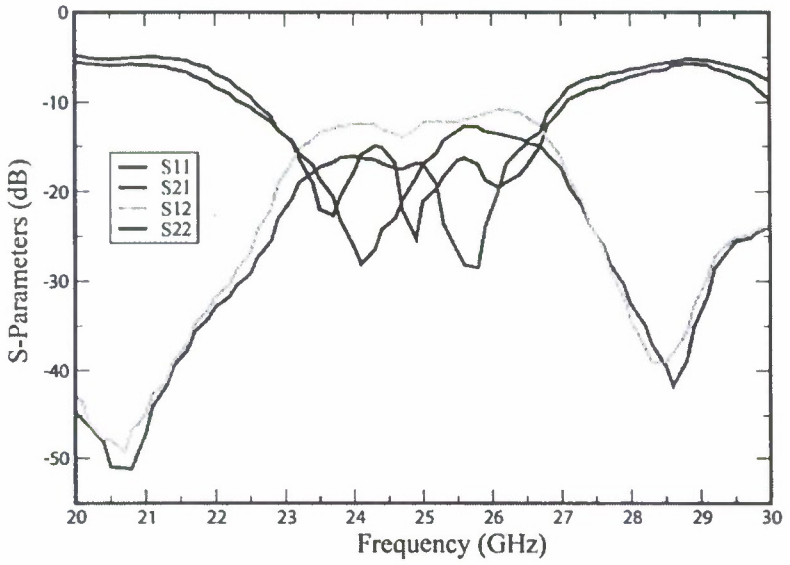

Fig. 5. S-parameter data for the circulator of Figure 3.

Since the network analyzer is a two-port instrument and the circulator is a three-port device, one of the ports was arbitrarily chosen to be terminated in a matched, 50 Ohm load. (Any port can be chosen since the device has geometrical symmetry.) The other two ports were connected to the network analyzer. In such a configuration, the network analyzer measures S_{11} (return loss, which is the relative strength of the reflected wave at port one), S_{12} (insertion loss, which is the attenuation of a signal traveling from port two to port one), S_{21} (isolation, which is the attenuation of a signal traveling from port one to port two) and S_{22} (return loss, which is the relative strength of the reflected wave at port two). In terms of dB, return losses and isolations of 14 dB or higher are desirable; insertion losses less than 1 dB are also attractive. The device is deemed highly non-reciprocal when $S_{12} \neq S_{21}$, which suggests that large discrepancies between the insertion loss and isolation have been achieved.

There are several interesting features in this data that deserve comment. First, we see a strong non-reciprocity effect in the vicinity of 25.8 GHz as seen in the spread of 17.0 dB

between S_{21} and S_{12}. Second, S_{21}, S_{11} , S_{22} exhibit good isolation and return losses performance of 28.5 dB, 17.0 dB and 12.7 dB, respectively. The adverse feature is the insertion loss associated with S_{12} of 11.7 dB. We surmise that this excessive insertion loss is due either to ferromagnetic linewidth broadening associated with the various shapes and sizes of the ferrite particles that comprise the mixture or to the epoxy

VI Conclusions

- During phase IV we achieve a complete fabrication of a BaM circulator by developing a novel composite material. This composite material allowed us to fabricate thick BaM films with a magnetization saturation $4\pi M_s$ between 2,000 to 2,500 Gauss, a perpendicular coercivity of 3,800 to 4,000 Oe and a squareness close to 0.9.
- The magnetic data demonstrates that a self-bias condition is achievable; the S-parameter data exhibits a strong circulator effect around 26 GHz. The one negative feature is the high insertion loss due to either linewidth broadening or to the epoxy used as a binder of the magnetic particles.

Bibliography

1. Zhuang, Z., Rao, M., White, R. M., Laughlin, D. E., Kryder, M. H.: J. Appl. Phys. 87, 6370 (2000)
2. Shinde, S. R., Ramesh, R.; Lofland, S. E., Bhagat, S. M., Ogale, S. B., Sharma, R. P., Venkatesan,T.: Appl. Phys. Lett. 72, 3443 (1998)
3. Donahue E. J., Schleich D. M., Thin solid films, 350, 119 (1999)
4. Yuan, M. S., Glass, H. L., Adkins, R. L.: Appl. Phys. Lett. 53, 340 (1988)
5. Wang, S.G., Yoon, S. D., Vittoria, C.: J. Appl. Phys. 92, 6728 (2002)
   Kranov, A. Y., Abuzir, A., Prakash, T., McIlroy, D. N., Yeh, W. J.: IEEE Trans. Mag. 42, 3338 (2006)
6. Sergey, V., Patton, C. E., Wittenauer, M. A., Saraf, L. V., Ramesh, R.: J. Appl. Phys. 91, 4426 (2002)
7. Oliver, S. A., Yoon, S. D., Kozulin, I., Chen, M. L., Vittoria, C.: Appl. Phys. Lett. 76, 3612 (2000)
8. Oliver, S. A., Shi, P., Hu, W., How, H., McKnight, S. W., McGruer, N. E., Zavracky, P. M., Vittoria, C.: IEEE Trans. Microwave Theory and Techniques, 49, 385 (2001).
9. O'Neil, B., Young J., Antennas and Propagation International Symposium and USNC/URSI National Radio Science Meeting, San Diego, California, July 2008.

Appendix B

FMR Spectrometer Upgrade to U-band Frequencies and Inter-laboratory Comparison at 52, 55, and 58 GHz

Dr. Nan Mo, Mr. Jaydip Das, and Dr. Carl E. Patton
Department of Physics, Colorado State University

I. Overview

In 2007/2008 under a subcontract to the University of Idaho (UI), the Colorado State University (CSU) team assisted the UI team in the upgrade of their FMR spectrometer system from X-band frequencies to U-band frequencies, that is, up to the range of 40 - 60 GHz, by replacing the X-band microwave components with U-band counterparts. A bi-laboratory comparison was carried out to verify the performance of this upgraded system. The intercomparison results show that (1) the system is functional and the FMR signal has a good signal-to-noise ratio, (2) the system can provide accurate FMR field and linewidth measurements at 40 - 60 GHz on standard ferrite samples, (3) the system can be configured to provide better performance if additional isolators are utilized to minimize microwave interference effects, and (4) anomalous resonances were observed in Barium ferrite thin films and granular thin discs. A theory has also been developed to make phase corrections in the FMR lock-in signal relative to the field modulation signal.

This report is to serve as the final report on the bi-laboratory comparison as well as the final report on the overall CSU subcontract.

II. Objectives:

The recent increasing need for low loss and high frequency magnetic devices, such as isolators, phase shifters, circulators, filters, delay lines, magnetic recording devices, and radar, has provided an impetus to renew the fundamental understanding of microwave loss and relaxation, damping processes, and precessional dynamics in magnetic materials. Ferromagnetic resonance (FMR) and the FMR linewidth have long been the mainstay for such studies. The University of Idaho (UI) established an initial Phase I subcontract with Colorado State University (CSU) that ended in 2006. In that project, a functional X-band FMR spectrometer system was constructed based on the shorted waveguide and lock-in techniques. The working frequency was 7-12 GHz.

A new Phase II subcontract was established in late 2006 that extended through June 2008. The objective herein was to upgrade the FMR spectrometer system from X-band to mm-wave frequencies (U-band). The operating mode for the initial Phase I system was configured for essentially any frequency range. Basically, one simply needs to replace one set of components for one band with another. In this specific case, one must replace the X-band components of this system with the U-band counterparts. The replaced components mainly include microwave source, waveguide system with short and isolator,

diode for detection, coaxial cables, and so on. As now completed, the operating frequency of the new system is in the U-band range, namely 40-60 GHz.

For such a high frequency range, the hardware and installation are critical. For the verification that the upgraded system runs properly, a CSU-UI interlaboratory comparison was done at the end of the program. The results show that the UI system can provide measurements consistent with the well-established CSU system.

More details about the upgrade and intercomparison are provided below.

III. U-band Frequency Upgrade of FMR Spectrometer System

A fully functional compact FMR spectrometer system was constructed at University of Idaho in 2006. This system utilized a waveguide short with the FMR signal detected based on field modulation and lock-in technique. For the details of working principles and operation, refer to "lock-in detection approach" in Appendix F of the 2006 report on the previous CSU subcontract from UI.

Now this system has been successfully upgraded to the frequency range from 40 to 60 GHz. The main changes are in the microwave components including microwave source, waveguide-to-coaxial-cable adaptors, high frequency coaxial cable, waveguides, isolators, waveguide short, diode detector, etc. Figure 1 shows photographs of the upgraded FMR spectrometer at UI. The key replacements consist of (1) vector network analyzer as a microwave source, (2) WR-19 waveguides for propagation of U-band microwave power, (3) 3 dB directional coupler that operates at U-band frequencies, (4) a special waveguide short with variable tuning of the position of the short, and (5) a waveguide-type broadband (full U-band frequency range) diode detector. It should be noted that the variable short is typically needed for mm-wave frequency so as to obtain a maximal FMR signal and improve the signal-noise ratio.

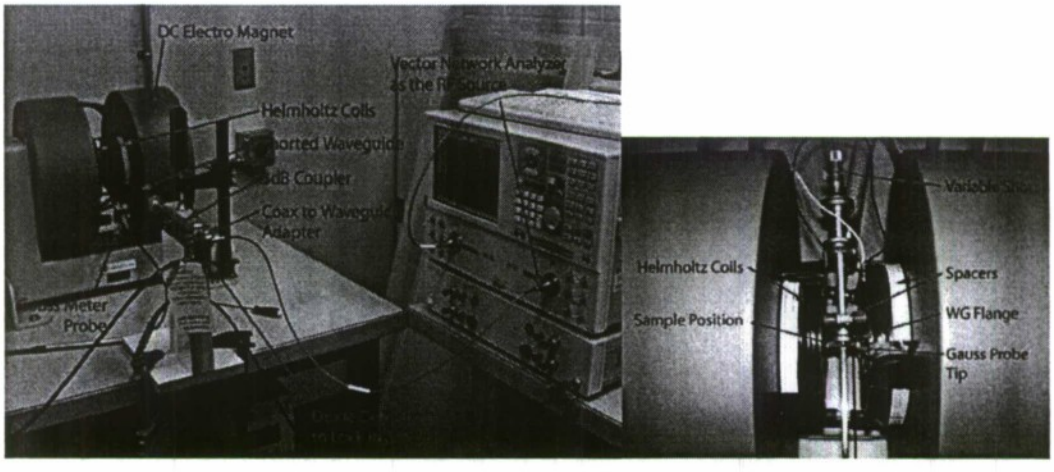

FIG. 1. Ferromagnetic resonance spectrometer system at the University of Idaho. The left image shows the full waveguide system and microwave source equipment. The right image shows the key detection part of the system, namely the waveguide short in magnet gap.

The Colorado State University provided the technical design and prototype testing at a nearly parallel in-house system at CSU and advising assistance to the UI team for the upgrade. The University of Idaho team was responsible for the hardware and system test at UI.

Figure 2 shows example FMR data from the UI system. These data were obtained on a granular barium ferrite thin disk. The blue open circles and yellow crosses show the in phase and out of phase FMR signals relative to the modulation signal.

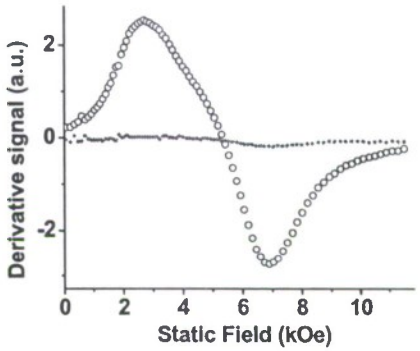

FIG. 2. Example FMR data obtained in a preliminary test by University of Idaho.

These data show a clear derivative FMR signal. The field difference from the low field peak to high field dip can be evaluated as the peak-to-peak linewidth. It is also evident from the data that the FMR signal shows a generally smooth response with a shape that shows only minor departures from the standard derivative Lorentzian form expected for small homogeneous samples. This means that the upgraded system has a good signal-noise ratio and a reasonable resolution. The low field wiggles likely come from the fact that the disk is not fully saturated.

IV. Bi-laboratory Intercomparison of mm-wave FMR

For verification and confirmation of the upgraded system performance, the CSU and UI teams decided to perform an interlaboratory comparison.

Interlaboratory comparisons are one of common means of determining the testing performance of a laboratory or an instrument together with proficiency of the testing operators. The results of intercomparison typically provide a basis for mutual recognition across worldwide testing laboratories. Although the CSU and UI laboratories focus is on magnetics research and not services, such an intercomparison is still useful to establish consistency and double check results for possible publication.

The CSU laboratory (Dr. Nan Mo) directed this bi-laboratory intercomparison and prepared the *Guidelines* (available upon request) that assure that the measurements at CSU and UI are performed under the conditions that form a valid basis for comparison.

The intercomparison was made basically as planned in the *Guidelines*. However, there were two unexpected changes. (1) The UI sample was broken prior to the return test by the UI laboratory. Subsequently, this second test was not done. Although tests on some other similar samples continued, those results are not reported here. (2) For the UI sample, the CSU laboratory observed a few sharp resonances that do not comprise the

usual FMR or spin wave resonance response. These anomalous resonances have been found to be consistent with some previous data obtained by Dr. Young-Yeal Song. The related physics of these effects will be one subject for future work.

More details are provided below.

A. Actual Samples

The thin Ba-ferrite film sample for the tests was provided by CSU. Dr. Jaydip Das prepared this sample by standard pulsed laser deposition (PLD) techniques. Figure 3 shows representative hysteresis data. These data give a saturation magnetic induction $4\pi M_s \approx 4.2$ kG and an effective uniaxial anisotropy field $H_u \approx 16$ kOe. This thin film is 0.5 μm in thickness, 6.8 mm^2 in area, and is close to rectangular in shape. The film is epitaxial but the easy uniaxial anisotropy axis likely shows some dispersion. Due to inhomogeneity line broadening and two magnon scattering losses, the FMR linewidth is expected to be significantly larger than the intrinsic linewidth for Ba-ferrite single crystals.

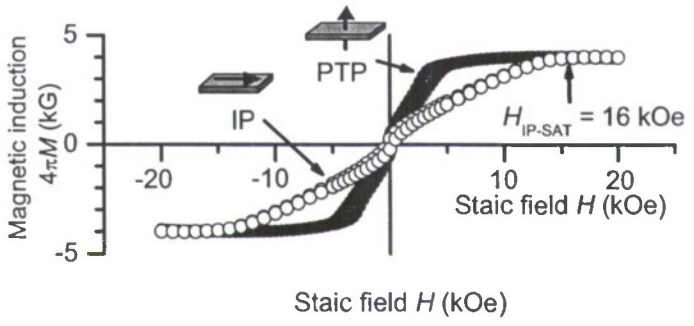

Fig. 3. Hysteresis loops for the thin Ba-ferrite film prepared by Dr. Jaydip Das using the pulsed laser deposition techniquc.

A thin Ba-ferrite disk sample with a rectangular shape was provided by UI. Thc disk is 0.24 mm in thickness and the area is about 7 mm^2. The sample was mounted on a 0.16 mm thick glass substrate. Figure 4 shows the hysteresis data. Effectively, it gives a saturation magnetic induction $4\pi M_s \approx 2.2$ kG (at a static field of about 12 kOe) and a uniaxial anisotropy field $H_u \approx 16.4$ kOe. It is known that the saturation magnetic induction is around 4.5 kG for standard barium ferrite. It is clear, therefore, that the real saturation magnetic induction of the disk is not 2.2 kG. It is evident that the disk is not saturated at the

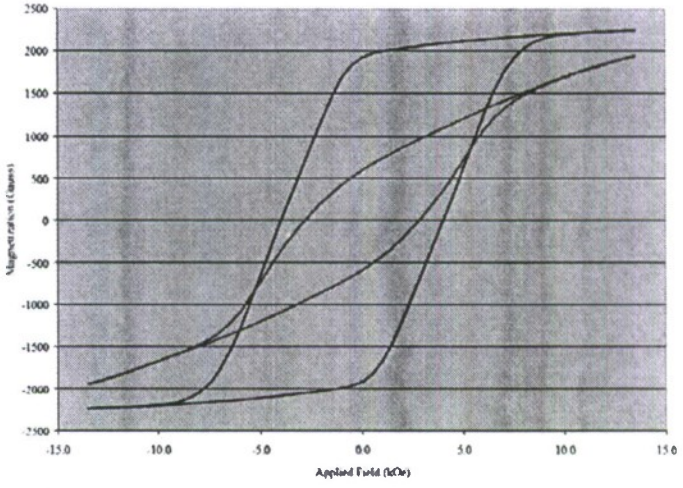

Fig. 4. Hysteresis loops for the thin Ba-ferrite disk provided by UI. The blue and red curves are for perpendicular and parallel magnetized cases, respectively. The vertical coordinatc is actually magnetic induction.

highest field (1.4 kOe) in Fig. 4. Onc can understand this if one examines thc microstructure, as shown bclow.

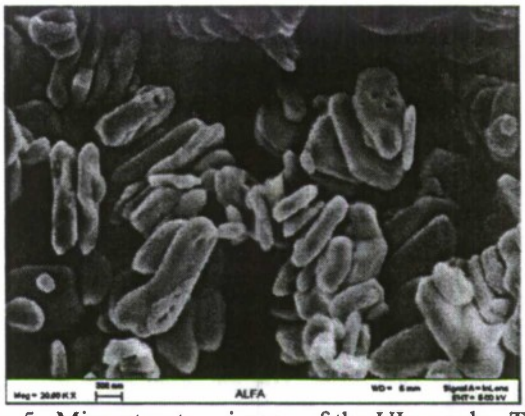

Fig. 5. Microstructure image of the UI sample. The wide slices are Ba-ferrite platelets.

The UI sample is made up of Ba-ferrite powder and an epoxy binder (nonmagnetic). Figure 5 shows the microstructure. The grains are generally comprised of thin slice like hexagonal platelets. This is because Ba-ferrite crystals have a hexagonal lattice structure. Thc grain size and orientation appear randomly distributed. One can expect that this kind of inhomogeneity results in a very large line broadening based on two facts: (1) the uniaxial anisotropy axes of the grains scatter in the full solid anglc range and the effcctive anisotropy field in cach grain is huge, around 16 kOe; (2) the platelet orientations also vary in the full anglc range relative to the applied ficld direction and corresponding magnetization direction for a saturated sample. The second effcct will scale with the crystalline value of $4\pi M_s$. The fact that the sample is not saturated exacerbates the inhomogeneity situation.

As mentioned above, the microstructure is also useful for the explanation of that the magnetization is not saturated at 1.4 kOe. There are always many grains whose orientations deviate from the direction of applied field. For these grains, the saturation field should be bigger than the effective anisotropy field (16.5 kOe) according to the Stoner-Wolfforth rotation model.

B. Data Analyses

Dr. Nan Mo made a MathCAD program (available upon request) for the calculation of FMR field and linewidth from raw data on the derivative of the resonance absorption vs. applied field profile. This program was used by both of the CSU and UI laboratories. This program includes two parts. (1) Pages 1-2 show the calculation for the magnetostatic spin wave dispersion relations. The zero wave number (k) limit corresponds to the FMR point. This calculation will prcdict the FMR position and also provide some partially explanation of the physical origins of the asymmetrical shape of the FMR signal. (2) Pages 3-5 do the FMR fitting. The fitting is to the derivative of a standard Lorentzian function. In practice, a constant background is added to this function so as to eliminate the systematic shift due to other effects of the spectrometer system. The final fitting function is nonlinear. Therefore, one should carefully choosc the initial values of fitting parameters. One should also carefully choose the field rangc for fitting. This is because spin wave resonances, particularly for thin films, may be very close to thc FMR signal; the program only works for one resonance at one time. Although this

program can be used for analyses of the spin wave resonances, such analyscs have not been done here.

Figure 6 shows an example of the FMR fitting. The data were obtained by CSU on the thin film sample at 58 GHz. The red open circles represent data points and the blue eurve show the derivative Lorentzian fitting. Thc symbols H_{max} and H_{min} indicate the high and low ficld points of the fitting range.

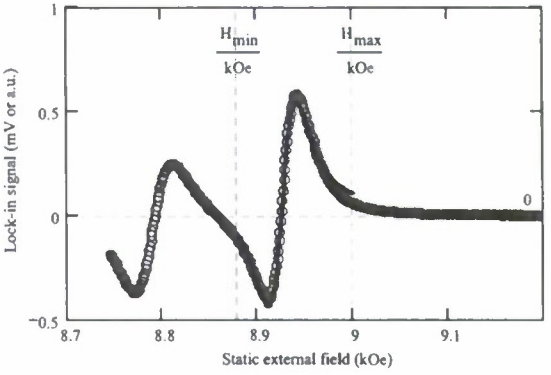

Fig. 6. Example for FMR fitting.

The University of Idaho also did a simple evaluation of the peak-to-peak linewidth and the FMR field by localizing the ficld positions of peak and dip.

C. Intercomparison Results

The CSU measurements werc performcd by Dr. Jaydip Das with Dr. Nan Mo's assistance. The UI measurements were performed by Mr. Benton O'Neil. Thc CSU and UI laboratories reported the results to eaeh other at the early of November 2007 as expeeted in the *Guidelines*. Diseussions and more tests continued up to June 2008. In this step, it should be noted that Dr. Young-Yeal Song at CSU was also involved in the analysis. Dr. Nan Mo presented the results in the meeting of Professors in November 2007. After thc meeting, Dr. Song was interested in the anomalous sharp peaks and showed the group some previous results on thin Ba-ferrite films that also had a clear signature with similar rcsonances at low fields. The details are provided in Sec. V.

C.1 Direct Comparison - Thin Film

Figure 7 shows representative FMR signals obtained by CSU and UI at 55 GHz. The thin film sample was measured first by CSU, as indicated by "CSU-1st Run." Then the sample was sent to UI for measurements, as indicated by "UI" and open squares. Finally, the sample was returned back to CSU, as indicated "CSU-2nd Run." The CSU 2nd run test was made for the confirmation that the internal properties of the sample didn't change during the two deliveries.

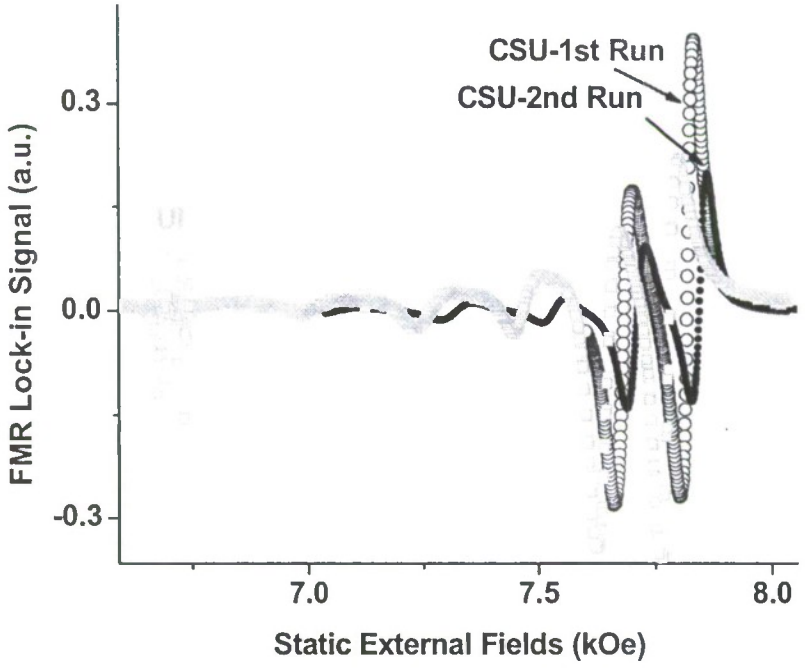

Fig. 7. Direct comparison of FMR signals on the CSU thin film sample at 55 GHz.

This direct comparison shows three points. (1) There is a FMR field shift among these three tests. The resonances with a highest field is the FMR signal. The FMR shift does not come from any change of the sample properties or any system instability. A few tests were done continuously without any change of the full system including the sample installation. The results show that there is almost no change in FMR fields. Another set of tests were also done by reinstalling the sample. The data, however, demonstrated a FMR field shift similar to Fig. 7. Therefore, such a shift is from sample mounting. Based on naked-eye adjustment, one usually mounts the sample and determines whether the sample position and waveguide orientation are in the right place. This will cause a variation of the angle between the normal of the sample and the static field, which then leads to a FMR field shift due to the variations in the components (along three directions of coordinates) of anisotropy field and demagnetizing field. If one wants to accurately compare the FMR fields for different thin film or disk sample, one should mount the sample with high precision, especially for high anisotropy and perpendicular magnetized

materials. Additionally, the Gaussmeter calibration and Hall probe installation may also contribute to the difference between CSU and UI's FMR field results.

(2) The line shapes between the CSU 1st run and 2nd run are about the same; these line shapes have a clear difference compared with UI results. Further discussions among these two laboratories come to the same point. Such a difference is from the system deformation. There are three possible contributions. The first is purely system related. Unlike the CSU system, the upgraded UI system does not utilize isolators. This leads to interference effects due to microwave reflection signals related to connection mismatches among waveguide components and coaxial cables as well.

The second lies in the field dependent linewidth (or effective linewidth). It will be easy to understand this point based on the spin wave dispersion curves that are shown in Fig. 8, as an example. In Fig. 8, the blue and red curves show the spin wave frequency vs wave number for spin waves propagating along the X- and Y- axes in the film plane. It is independent on how the coordinates are chosen. The dashed red line indicates the pumping frequency and also the FMR frequency. Above FMR frequency or below FMR field, there are degenerate spin waves (or magnon) with the uniform mode (that always exists due to a finite FMR linewidth in reality). This will induce the well-developed two magnon scattering processes. On the other hand, below the FMR frequency or above the FMR field, there are no degenerate spin wave modes and no two magnon scattering processes exist. The above comes to the point that the FMR relaxation and linewidth at low fields is larger than that at high fields. The fact that the height of low field dip is less than the one of high field peak for CSU data is the evidence for such field dependence. Generally speaking, the linewidth is field dependent.

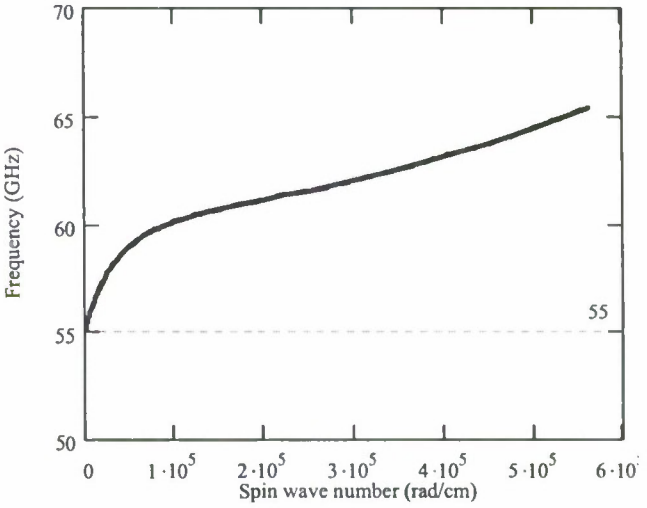

Fig. 8. Dipole-exchange magnetostatic spin wave dispersion curves.

To resolve the second problem, one should refer to the effective linewidth technique (see Nan Mo, Ph.D. dissertation, Colorado State University, 2006). Typically, the effective linewidth determination requires microwave cavity measurements. Dr. Nan Mo also tried to extract the effective linewidth from the above FMR lock-in signal. Theoretically, this is possible. However, one needs to eliminate the systematic deformation of this signal and precisely determine the constant background. This is extremely important for the high field regime because the signal is very small and any error will result in huge systematic errors in effective linewidth.

The third is that the errors in the phase between FMR signal and modulation signal could also contribute the difference. This is because the actual phase depends on the sample insertion and the susceptibility of material that is field dependent. Such field dependence requires an extra phase correction. Mr. Benton O'Neil developed the full theory for this phase correction. However, such a correction procedure was not applied to the data analyses as a part of this intercomparison.

(3) The UI measurements that covered a wider field range than CSU show a few resonances below around 6.5 kOe. To the knowledge of the CSU and UI group members, these resonances have never been reported in literature. In this report, such observations are taken as an anomaly and will be discussed in more details in Sec. V.

C.2 Direct Comparison - Nearly Square Thin Disk

Figure 9 shows the representative FMR signals on thin disks obtained by CSU and UI at 55 GHz. The thin disk sample was measured first by UI, as indicated by "UI" and open squares. Then the sample was sent to CSU for measurements, as indicated by "CSU" and

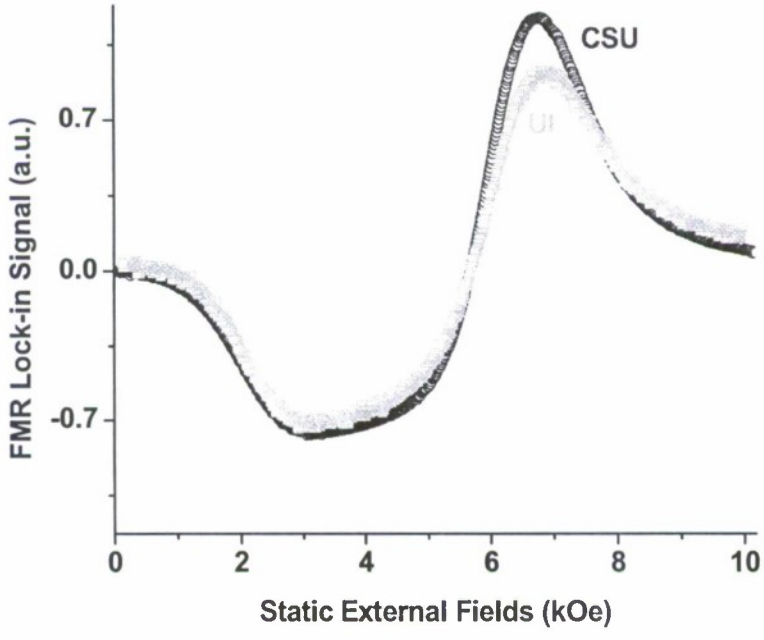

Fig. 9. Direct comparison of FMR signals on the UI thin disk sample at 55 GHz.

open circles. Finally, the sample was returned back to UI, but no data are shown here because the sample was broken when UI personnel removed the tapes attached on the sample. The missing of the UI 2nd run test can be ignored. The sample was handled with extreme carefulness. In Fig. 9, the UI data are scaled so that the UI and CSU signal has comparable amplitudes. It is evident that both sets of data show a very smooth response that is a signature for a good signal-noise ratio. One also sees that these two line shapes are nearly the same except for the relative shorter height of the high field peak

for the UI measurement. However, the line shapes show a clear deviation from the standard derivative Lorentzian curve. Specifically, the low field dips are very broad compared to the high field peaks. This is because the sample is not saturated even at 4.5 kOe (see Fig. 4). The lack of saturation leads to a field dependent FMR field shift and extra low field loss. These effects cause a distortion in the FMR signal of the sort in evidence here. Finally, it should be noted that the FMR linewidth is very large, on the order of 3 kOe, as expected from the microstructure data and the corresponding inhomogeneous linebroadening and two magnon scattering considerations discussed in connection with Fig. 5.

The best way to evaluate the FMR field and linewidth is to determine the dip (lowest) and peak (highest) fields at the extrema of the derivative absorption profile. Their average and difference give the FMR field and peak-to-peak linewidth, respectively. From visual inspection of Fig. 9, one can see that the CSU and UI results for linewidth and position are about the same. Any more precise comparison is not meaningful because of the low field distortion and the large linewidth, as mentioned above.

C.3 Comparison of FMR Results - Thin Film

Tables I and II list the FMR field and linewidth results, respectively, reported by CSU and UI on the CSU Ba-ferrite thin film sample. Specifically, the last columns show the values of the average of CSU 1st run and 2nd run minus the UI results. These results are plotted in Fig. 10. It should be emphasized that for the CSU FMR results, only the Type A uncertainty (termed random error) is listed. The Type B uncertainty (termed systematic error) can be evaluated as 25 Oe because this is the tested variation of Gaussmeter readings by remounting the Hall probe many times. [Note that trained metrologists typically avoid the terminology "random error" or "systematic error." This is because systematic effects for a set of specific measurement can also cause a random distribution of measurement results if measurements are made in for wide range of systems, ambient conditions, and operators.]

Table I. FMR field data

Frequency (GHz)	CSU 1st Run (Oe)	UI (Oe)	CSU 2nd Run (Oe)	Difference (Oe)
52	6781±4 (type A)	6723 ±51	6802±4 (type A)	68.5
55	7863.5±4 (type A)	7795±83	7890±4 (type A)	82
58	8926±1.3 (type A)	8858±67	8964.5±4 (type A)	89

Table II. FMR linewidth (half maximum) data

Frequency (GHz)	CSU 1st Run (Oe)	UI (Oe)	CSU 2nd Run (Oe)	Difference (Oe)

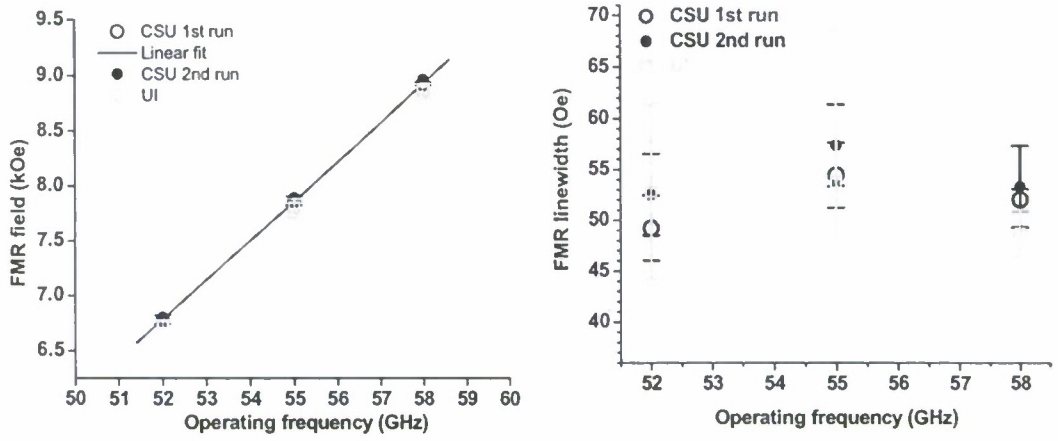

Fig. 10. Plots of the results in Tables 1 and 2. These graphs are self indicated.

52	49.2±1.6	52.8±8.6	52.5±1.6	-2.0
55	54.4±1.6	53.7±14.9	57.4±1.6	2.2
58	53.0±1.6	48.7±2.3	53.3±1.6	4.5

(1) FMR field

After the consideration of the Type B uncertainty, all of the FMR field differences between CSU and UI as shown in the last column of Table I are in the range of the error bars. This certifies the validity of the measurement capability of the UI laboratory and the good performance of the UI system. As discussed above, the main errors come from two Type B uncertainties. One is due to the sample installation and waveguide orientation. The other is due to the Hall probe installation. The more careful treatment on these two dominant uncertainty sources will reduce the total uncertainties.

The FMR field vs frequency response shows a linear dependence; see the left graph in Fig. 10. This is the expected result for any perpendicular magnetized thin film.

(2) FMR linewidth:

The two dominant uncertainty sources do not make any contribution to the uncertainty of FMR linewidth measurements because in principle the linewidth value is always the difference between the two points at the half maximum of the integral curve of the lock-in signal. In Fig. 10, right side graph, there are overlaps among the CSU and UI uncertainty ranges at all three different operating frequencies. So, the linewidth measurements at UI are highly consistent with CSU. This may be because the "systematic errors" do not contribute to the scattering of the linewidth data points.

V. ANOMALOUS OBSERVATIONS

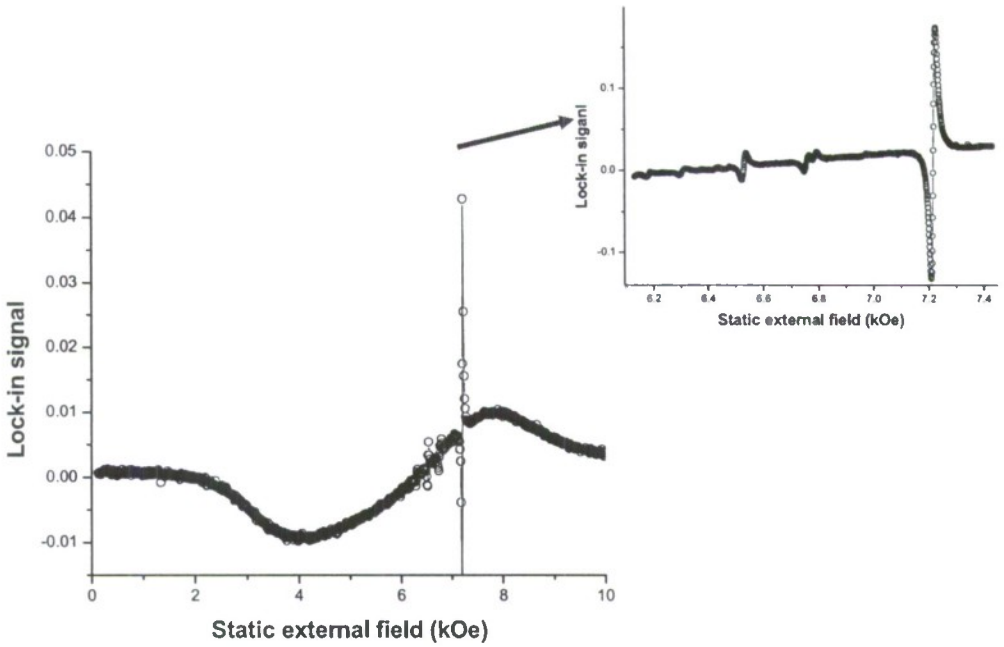

Fig. 11. The careful measurements on the UI thin disk sample. The right graph is for the step field that equals to 5 Oe. The left graph is for a smaller step field of 2 Oe.

When Dr. Jaydip Das and Nan Mo took the measurements on the UI thin disk sample with a step field of 10 Oe, as reeommended in the *Guidelines*, there were often a few diserete points that show a pronounced departure from the line shape obtained from the other large number of points. These points appear to be bad points because of a malfunetion of the spectrometer system. A full check was made on the system components and Labview program. However, the check showed that these points were all sample related. The eareful set of 58 GHz measurements were then made; these are shown in Fig. 11.

It appears that near 7.3 kOe there are a few extra narrow resonanees. The linewidth of the strongest amplitude resonance is 28 Oe (absorption eurve half maximum) and 16 Oe (peak-to-peak absorption eurve derivative linewidth). This linewidth is the same as the best for the PLD Ba-ferrite films, refer to "*Optimized pulsed laser deposited barium ferrite thin films with narrow ferromagnetic resonance linewidths*," Y. Y. Song, S. Kalarickal, and C. E. Patton, J. Appl. Phys. 94, 5103-5110 (2003). This is a surprising observation. It appears that the random grain sizes and orientations do not serve, for some reason to wash out these narrow peaks. At the same time, one also sees an overall FMR linewidth is around 3 kOe that clearly is a signature of inhomogeneity line

broadening due to the random variation in grain size and orientation. Further system tests without sample proved that these resonances do come from the magnetic sample.

Dr. Young-Yeal Song continued several tests on this anomalous behavior. The main conclusions based on his results are (1) that these resonances are magnetic because the ratio of frequency to resonance field equals to the gyromagnetic ratio and (2) that those resonances have the same origins as the resonances that appear near 6.5 kOe in Fig. 7. Further work is needed on this effect. It may be due to the simple FMR response of large grains that show up independently of the overall response.

VI. FUTURE WORK

In the event that further support is obtained from ONR for the CSU program, further investigations will be made on (1) the anomalous observations to solve the corresponding theoretical and experimental problems and (2) the development of simplified effective linewidth technique for Ba-ferrite materials based on high precision FMR lock-in detection methods.

Appendix C

Experimental Investigation of a Self-Biased Microstrip Circulator
Mr. Benton O'Neil and Dr. Jeffrey L. Young

The attached document was originally published in the *IEEE Transactions on Microwave Theory and Techniques*, vol. 57, no. 7, pp. 1669-1674, 2009. The document discusses all the important findings of the Microwave Group during Phase IV.